



## Late Pleistocene zircon ages for intracaldera domes at Gölcük (Isparta, Turkey)



Axel K. Schmitt<sup>a,1</sup>, Martin Danišik<sup>b,\*</sup>, Wolfgang Siebel<sup>c</sup>, Ömer Elitok<sup>d</sup>, Yu-Wei Chang<sup>e</sup>, Chuan-Chou Shen<sup>e</sup>

<sup>a</sup> Department of Earth, Planetary, and Space Sciences, University of California, Los Angeles, 595 Charles Young Dr., Los Angeles, CA 90095-1567, USA

<sup>b</sup> Faculty of Science & Engineering, University of Waikato, Private Bag 3105, Hamilton 3240, New Zealand

<sup>c</sup> Department of Geosciences, Universität Tübingen, Wilhelmstr. 56, 72074 Tübingen, Germany

<sup>d</sup> Department of Geological Engineering, Süleyman Demirel University, 32260 Isparta, Turkey

<sup>e</sup> High-Precision Mass Spectrometry and Environment Change Laboratory (HISPEC), Department of Geosciences, National Taiwan University, Taipei, Taiwan, ROC

### ARTICLE INFO

#### Article history:

Received 28 April 2014

Accepted 23 August 2014

Available online 4 September 2014

#### Keywords:

Anatolian Plate

Post-collisional volcanism

Trachyte

Uranium series

(U–Th)/He

### ABSTRACT

Pleistocene to Quaternary volcanism in the Isparta region (SW Anatolia, Turkey) comprises potassic lavas and pyroclastic deposits, which are largely centered around Gölcük caldera. Trachytic intracaldera lava domes represent the latest eruptive event at Gölcük, and their eruption age is crucial for defining a minimum age for the preceding caldera-forming explosive eruption. Here, we present combined U–Th and (U–Th)/He zircon geochronological data for two intracaldera lava domes constraining their crystallization and eruption ages, respectively. U–Th zircon crystallization ages peak between ca. 15 and 25 ka. In rare instances U–Th zircon crystallization ages date back to ca. 59 and 136 ka. U–Th zircon crystallization ages also permit (U–Th)/He eruption ages from the same crystals to be individually corrected for uranium series decay chain disequilibrium, which is mainly due to the deficit of the intermediate daughter <sup>230</sup>Th in zircon. Average disequilibrium-corrected (U–Th)/He zircon ages are  $14.1 \pm 0.5$  and  $12.9 \pm 0.4$  ka (1 $\sigma$ ). These ages are indistinguishable within analytical uncertainties suggesting that both lavas erupted quasi simultaneously. This contradicts published K–Ar ages that suggest an extended hiatus from ca. 52 to 24 ka between intracaldera dome eruptions. Evidence for protracted zircon crystallization over several thousands of years prior to eruption indicates the presence of a long-lived magma reservoir underneath Gölcük caldera. Implications of the revised eruptive geochronology presented here include younger ages for the latest effusive eruptions at Gölcük, and potentially also a more recent explosive eruption than previously assumed.

© 2014 Elsevier B.V. All rights reserved.

## 1. Introduction

Gölcük (Isparta Region, Turkey) volcano is a multi-cycle eruptive center with a prolonged history of explosive and effusive eruptions throughout the Pleistocene (Alici et al., 1998; Platevoet et al., 2008; Elitok et al., 2010). An important consideration for volcanic hazards is that these deposits extend into and beyond the city limits of modern Isparta with a population of ~200,000. Obtaining reliable eruption ages for the youngest Gölcük effusive eruptions is important because they provide minimum age constraints for the preceding explosive cycle and are essential for better assessment of future eruptions of a volcano in close proximity to a densely populated urban region. Mapping and reconnaissance-level K–Ar (Ar–Ar) geochronology has identified at least three eruptive cycles (Alici et al., 1998; Platevoet et al., 2008). The youngest of these cycles initiated with a phreatoplinian phase whose deposits blanket the flanks of

the volcano, and form a gently sloping apron towards the N centered around a ~2.5 km diameter maar-type crater now partly filled by a lake (Fig. 1). Subsequent to the explosive caldera-forming eruption, small-volume lava domes erupted inside the crater, and these domes represent the youngest volcanic event at Gölcük.

Here, we revisit the dating of Gölcük lavas from the youngest eruption cycle and provide two independent, but mutually supportive, age constraints: U–Th zircon crystallization ages and (U–Th)/He zircon eruption ages. These ages are younger than previously published K–Ar ages for Gölcük lavas, and warrant a re-evaluation of the recent volcanic history of Gölcük volcano. The advantage of the geochronological approach followed here is that (U–Th)/He and U–Th ages can be scrutinized for internal consistency on a crystal-by-crystal basis which transcends conventionally employed Quaternary geochronometers such as those based on the K–Ar decay system.

## 2. Geologic setting

The Pliocene–Pleistocene deposits of Gölcük volcano form the most recent member in an eponymous series of intra-continental high-K volcanic rocks. We note that the term Isparta volcanic series has also been

\* Corresponding author.

E-mail addresses: [axel@oro.epss.ucla.edu](mailto:axel@oro.epss.ucla.edu) (A.K. Schmitt), [m.danisik@waikato.ac.nz](mailto:m.danisik@waikato.ac.nz) (M. Danišik), [wolfgang.siebel@uni-tuebingen.de](mailto:wolfgang.siebel@uni-tuebingen.de) (W. Siebel), [oelitok@mmf.sdu.edu.tr](mailto:oelitok@mmf.sdu.edu.tr) (Ö. Elitok), [oojohn1981@gmail.com](mailto:oojohn1981@gmail.com) (Y.-W. Chang), [river@ntu.edu.tw](mailto:river@ntu.edu.tw) (C.-C. Shen).

<sup>1</sup> Tel.: +1 310 206 5760; fax: +1 310 825 2779.

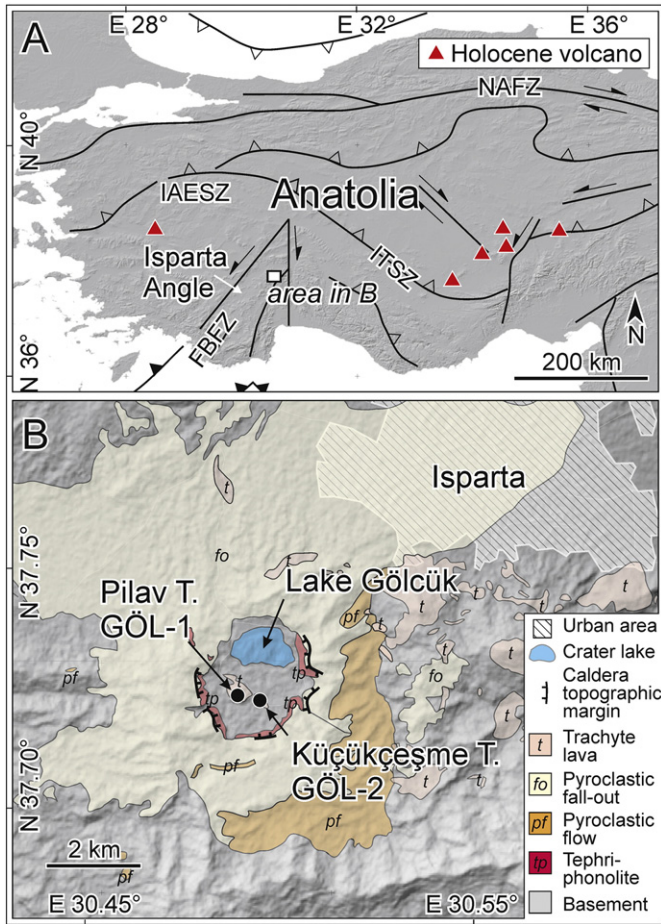


**Fig. 1.** Location map of the Gölcük volcanic field (A) in comparison with recent volcanoes in Anatolia, and major tectonic units (open triangles: sutures; closed triangles: subduction thrusts; solid lines: transform faults). Simplified geologic map of the central Gölcük volcanic field (B), indicating the sampling locations for intracaldera trachyte domes. NAFZ – North Anatolian Fault Zone; IAESZ – İzmir-Ankara-Erzincan Suture Zone; ITSZ – Inner Tauride Suture Zone; FBFZ – Fethiye Burdur Fault Zone. Basement rocks comprising various autochthonous and allochthonous units are shown undivided.

used in the literature because of the close proximity (~7 km) of Isparta city center to the main crater (Fig. 1; Supplementary Data). The Gölcük volcanic series extends over an area of ~100 km<sup>2</sup> and it is located near the northern cusp of the Isparta Angle (Fig. 1), a major orocline located at the northward projection of the intersection between the Hellenic and Cyprus arcs (Dilek and Sandvol, 2009). Differential convergence rates between Anatolia and the African lithosphere, fast for the Hellenic and slow for Cyprus arc, may have resulted in slab tear with decompressional melting in the asthenosphere due to upwelling in the region of the Isparta Angle (Dilek and Sandvol, 2009). Gölcük magmas are exceptionally potassic compared to other post-collisional volcanic provinces that exist in the hinterland of Tethyan suture zones (Elitok et al., 2010; Dilek et al., 2010), and include lamprophyres and basanites derived from melting of previously subduction-metasomatized lithosphere (Elitok et al., 2010; Platevoet et al., 2014). Country rocks that are intruded or overlain by Gölcük volcanic deposits include Mesozoic to lower Cenozoic allochthonous limestone and ophiolitic mélangé overthrust onto lower Miocene sandstone and shale (Ağlasun formation) and post-collisional Middle–Upper Miocene Gönen conglomerates (Alici et al., 1998; Elitok et al., 2010). Isotopic variation over the Gölcük lavas and pyroclastic rocks ( $\text{SiO}_2 = \sim 52$  to 66 wt.%) is minor (modern values:  $\epsilon_{\text{Nd}} = 0$  to +2;  $^{87}\text{Sr}/^{86}\text{Sr} = 0.7037$  to 0.7050), but higher  $^{87}\text{Sr}/^{86}\text{Sr}$  correlating with increasing fractionation suggests that magmas evolved while undergoing crustal assimilation

during ascent through thick (~30–40 km) continental crust (Alici et al., 1998; Elitok et al., 2010).

The earliest dated volcanic rocks of the Gölcük series are Pliocene leucitites with K–Ar ages of  $4.7 \pm 0.50$  Ma (1 $\sigma$ ; hereafter) and  $4.07 \pm 0.20$  Ma (Lefèvre et al., 1983). Eruptions of Gölcük sensu stricto have been grouped into three phases (comprising cycles I to III from older to younger; Platevoet et al., 2008). Dating mesostasis from lavas by the unspiked K–Ar method yielded ages of  $2.77 \pm 0.06$  Ma for an eroded trachyandesite dome, and  $115 \pm 3$  ka and  $62 \pm 2$  ka for tephriphonolite lavas exposed at the margin of the Gölcük crater, and define cycle I and cycle II eruptions, respectively (Platevoet et al., 2008). Preliminary  $^{40}\text{Ar}/^{39}\text{Ar}$  K-feldspar analyses from pumice yielded a wide spread of ages with minima of ca. 206 ka (cycle I) and ca. 54 ka (cycle III; Platevoet et al., 2008). These ages represent mixed phenocryst populations whose age significance is difficult to interpret.

The most recent eruptions comprise trachytic lavas inside the Gölcük crater that resulted in the extrusion of the conical Pilav Tepe dome which constrains a minimum age for the preceding cycle III crater-forming explosive eruption. Pilav Tepe is ~0.5 km in diameter at its base and emerges ~150 m above the modern lake level. A morphologically subdued (~50 m above modern lake level) lava flow or cryptodome named Küçükçeşme Tepe with dimensions of ~100 × 200 m abuts Pilav Tepe to the SE. Platevoet et al. (2008) reported K–Ar ages of  $52 \pm 2$  ka (Küçükçeşme Tepe; here sample GÖL-2) and  $24 \pm 2$  ka (Pilav Tepe; here GÖL-1) suggesting a protracted magmatic hiatus between these eruptions; this is rejected based on our results (see below).

Compositionally, Pilav Tepe and Küçükçeşme Tepe lavas are compositionally similar and slightly more evolved ( $\text{SiO}_2 \sim 61$  wt.%) than pumice erupted during the preceding explosive phase (~54 wt.%; Alici et al., 1998; Elitok et al., 2010). They also have slightly lower Zr abundances (~400 ppm) than cycle III pumice deposits (~500 ppm). These relations are typical for lavas and pumice from the Gölcük suite which display largely invariant Zr with increasing  $\text{SiO}_2$  up to ~60 wt.%, and only a mild decrease in Zr for rocks with higher silica content ( $\text{SiO}_2 = 60$  to 64 wt.%).  $\text{P}_2\text{O}_5$  by contrast continuously decreases approximately tenfold over the same  $\text{SiO}_2$  range. This strong depletion implies efficient apatite fractionation which is consistent with the presence of abundant accessory apatite over the entire compositional range (Alici et al., 1998; Elitok et al., 2010; Platevoet et al., 2014). In contrast to apatite, zircon appears to be much rarer in Gölcük volcanic rocks (Platevoet et al., 2014).

### 3. Material and methods

Several kilograms of rock were collected from the summit of Pilav Tepe (GÖL-1) and a small quarry at Küçükçeşme Tepe (GÖL-2; locations in Table 1). Both samples were excavated from ~20 cm depth, avoiding surficial rocks that might have experienced heating due to wild fires or lightning. Zircon was recovered using standard separation techniques, and large euhedral crystals were handpicked and pressed into indium (In) metal using an evenly machined tungsten carbide anvil so that zircon prism faces were level with the mount surface. Secondary ion mass spectrometry (SIMS) U–Th isotope analysis was performed by sputtering crystals perpendicular to their prism surfaces to a depth of ~5  $\mu\text{m}$  and lateral spot dimensions of  $\sim 20 \times 30 \mu\text{m}$ . Instrument parameters for the UCLA CAMECA ims1270 ion microprobe followed Schmitt et al. (2011). After these “rim” analyses, a subset of the crystals was extracted from the mounts, photographed, and packed into niobium tubes for (U–Th)/He analysis following protocols for noble gas (for  $^4\text{He}$  abundances) and inductively coupled plasma mass spectrometry (ICP MS) at Curtin University (Schmitt et al., 2011). Crystals that were not analyzed for (U–Th)/He were ground and polished using SiC and diamond abrasives to remove the outer ~20  $\mu\text{m}$  of the crystals. The exposed interiors were imaged using cathodoluminescence under electron beam bombardment in a Leo 1430VP scanning electron microscope in order to characterize the internal structures of the zircons (Supplementary

**Table 1**  
Results for combined U–Th and (U–Th)/He zircon analysis of Gölcük intracaldera domes.

Sample	<sup>232</sup> Th (ng)	±1σ (%)	<sup>238</sup> U (ng)	±1σ (%)	<sup>4</sup> He (ncc)	±1σ (%)	TAU (%)	Ft	Ft-Cor. Age (ka)	± (ka)	<sup>238</sup> U/ <sup>230</sup> Th age (ka)	± (ka)	D <sub>230</sub>	Diseq.-Cor. Age (ka)	+ (ka)	- (ka)
<i>GÖL-1 (N 37°43.328' E 30°29.322')</i>																
z-1	47.3	3.9	25.0	4.7	0.0531	4.4	5.6	0.86	14.1	1.1	58.9	9.1	0.55	16.5	1.1	1.4
z-3	21.0	3.9	11.1	4.3	0.0194	11.4	11.9	0.83	12.0	1.5	17.2	3.6	0.54	15.2	1.6	2.2
z-5	33.1	3.9	25.4	4.5	0.0368	6.1	7.1	0.89	10.3	0.9	38.2	7.3	0.38	13.8	1.1	1.4
z-6	44.2	3.9	32.5	4.6	0.0492	4.7	5.9	0.85	11.2	0.9	35.6	5.7	0.39	14.8	1.1	1.2
z-7	30.0	3.9	17.1	4.5	0.0245	9.1	9.7	0.83	10.0	1.1	32.0	3.9	0.50	12.2	1.5	1.2
z-8	12.9	3.8	9.6	4.2	0.0139	15.9	16.2	0.88	10.2	1.7	34.7	6.5	0.39	13.3	2.6	1.9
z-9	85.5	3.8	29.9	4.3	0.0693	3.4	4.6	0.88	12.9	0.9	62.4	7.6	0.82	13.3	1.0	0.8
Eruption age (average of disequilibrium corrected ages): 14.1 ± 0.5 ka (n = 7; Q = 0.47)																
<i>GÖL-2 (N 37°43.181' E 30°29.616')</i>																
z-1	21.0	3.9	18.7	5.1	0.0194	6.9	8.0	0.83	8.1	0.8	16.2	3.9	0.35	11.9	1.2	1.1
z-2	10.9	3.9	8.6	4.3	0.0070	18.7	19.0	0.82	6.3	1.2	9.8	3.0	0.39	9.4	1.4	2.1
z-3	30.2	3.9	21.2	4.5	0.0272	5.0	6.1	0.85	9.2	0.7	21.6	2.6	0.44	12.1	1.1	0.9
z-4	11.6	3.9	8.8	4.7	0.0077	16.9	17.3	0.85	6.5	1.2	22.6	4.2	0.41	8.5	1.8	1.3
z-7	39.1	3.9	26.6	4.7	0.0391	3.6	5.1	0.85	10.6	0.8	16.9	4.5	0.46	14.0	1.2	0.9
z-8	26.1	3.9	19.7	4.3	0.0332	4.1	5.4	0.88	12.0	0.9	29.3	5.3	0.41	16.2	1.0	1.4
z-9	55.5	3.8	24.7	4.6	0.0524	2.8	4.3	0.91	12.6	0.8	17.0	4.0	0.70	14.2	1.0	1.0
Eruption age (average of disequilibrium corrected ages): 12.9 ± 0.4 ka (n = 7; Q = 0.001)																

All data are for individual crystals; <sup>4</sup>He – volume of helium in ncc at STP; TAU – total analytical uncertainty; Ft – alpha retention factor (Farley et al., 1996; Hourigan et al., 2005); Ft-Cor. age – (U–Th)/He age corrected for alpha ejection; <sup>238</sup>U/<sup>230</sup>Th age – determined by SIMS (Supplementary Table 2); D<sub>230</sub> – Th zircon-melt fractionation factor (Farley et al., 2002); Diseq.-Cor. age – (U–Th)/He age corrected for disequilibrium.

data). Subsequently, they were analyzed for U–Th isotopic compositions as “interior” ages in the same fashion as the “rim” spots.

Whole-rock U and Th isotopes were analyzed after ion exchange chromatographic purification of the U and Th fractions from acid-digested rock powder by a triple-spike <sup>229</sup>Th–<sup>233</sup>U–<sup>236</sup>U isotope dilution on a multi-collector (MC) ICP-MS, Thermo-Electron Neptune, at the National Taiwan University (Shen et al., 2002, 2003, 2012).

Zircon crystallization ages were calculated as model ages in (<sup>230</sup>Th)/(<sup>232</sup>Th) vs. (<sup>238</sup>U)/(<sup>232</sup>Th) space, using the <sup>230</sup>Th half-life of Cheng et al. (2013). Magma composition as represented by the whole-rock U–Th isotope composition was used as a fixed point, and the (<sup>230</sup>Th)/(<sup>238</sup>U) slope was determined for individual zircon points. The individual rim zircon crystallization ages with their respective uncertainties were then used to correct (U–Th)/He ages for the effects of <sup>230</sup>Th deficit during zircon crystallization, that would otherwise lead to significant underestimation of true eruption age (Farley et al., 2002). Disequilibrium corrections also included subtracting <sup>4</sup>He produced by excess <sup>231</sup>Pa, but this is a very minor correction (Schmitt, 2007). All disequilibrium corrections were implemented using the MCHCalc software (with (U–Th)/He ages, uncertainties, and goodness-of-fit parameters calculated by fully propagating individual analytical uncertainties via Monte-Carlo simulations with 100,000 trials per sample (Schmitt et al., 2010a)).

## 4. Results

### 4.1. U–Th zircon crystallization ages

All zircon rims and interiors for samples GÖL-1 and GÖL-2 show <sup>230</sup>Th deficits (i.e., they plot to the right of the equiline; Fig. 2; Supplementary data). Both samples yielded indistinguishable model ages ranging between ca. 10 and 136 ka (rims), and ca. 11 and 56 ka (interiors). The majority of U–Th zircon ages fall between ca. 15 and 25 ka. No xenocrystic zircon crystals (with ages in secular equilibrium) were detected. Zircon U abundances (111–1660 ppm; average = 787 ppm) and Th/U (0.234–2.08; average = 1.16) are similar between rims and interiors, and lack coherent trends with age over the entire range of crystallization ages (Fig. 3). Th/U in GÖL-1 and GÖL-2 zircons is high compared to the zircon average of ~0.5 (Hoskin and Schaltegger, 2003). This reflects the elevated whole-rock Th/U of 3.32 (Fig. 3).

### 4.2. (U–Th)/He zircon eruption ages

The detection of ubiquitous uranium decay series disequilibrium in GÖL-1 and GÖL-2 zircon rims and interiors implies that (U–Th)/He zircon ages will underestimate the eruption age when deficits in <sup>230</sup>Th remain unaccounted. After correction for disequilibrium using the U–Th rim age constraints, (U–Th)/He zircon ages variably increase, depending on the initial deficit in <sup>230</sup>Th, and the duration of pre-eruptive crystal residence (Farley et al., 2002). In the case of GÖL-1 and GÖL-2 zircons, disequilibrium corrections increase the (U–Th)/He age by ca. 1 and 4 ka (or ~10 and 30%, relative), respectively (Fig. 4; Table 1). The averages for seven replicates per sample (Fig. 4) are 14.1 ± 0.5 ka (GÖL-1) and 12.9 ± 0.4 ka (GÖL-2) with goodness-of-fit parameters ≥ 10<sup>−3</sup> indicating uniform age populations for each sample (Press et al., 2002). The average ages of the two samples are within error, suggesting a (near-)coeval eruption of Pilav Tepe and Küçükçeşme Tepe. This is at variance with the previously reported 28 ± 2 ka age difference between K–Ar ages for the same pair of intracaldera domes (Platevoet et al., 2008).

## 5. Discussion

### 5.1. Comparison with published eruption ages

Disequilibrium-corrected (U–Th)/He zircon ages for two intracaldera lavas from Gölcük indicate (near-)coeval eruption at ca. 13 ka. This age is in agreement with the youngest U–Th zircon and whole-rock model ages, and consistent with pre-eruptive zircon crystallization which pre-dates the eruption by up to 150 ka. K–Ar ages published for the same lavas (Platevoet et al., 2008) are significantly older than the (U–Th)/He determined eruption age, and are also inconsistent with the U–Th zircon crystallization ages: 42% of U–Th zircon ages postdate the 24 ka K–Ar age at 95% confidence, and almost all U–Th zircon ages are younger than the older K–Ar age of 52 ka. Because zircon crystallization must predate eruption, it is implausible that U–Th zircon ages would be younger than K–Ar eruption ages. This fundamental conflict between U–Th zircon crystallization and K–Ar eruption ages is resolved when assigning the (U–Th)/He zircon ages as eruption ages.

(U–Th)/He zircon dating has yielded reliable ages for late Quaternary lavas which agree with age constraints from other geochronological

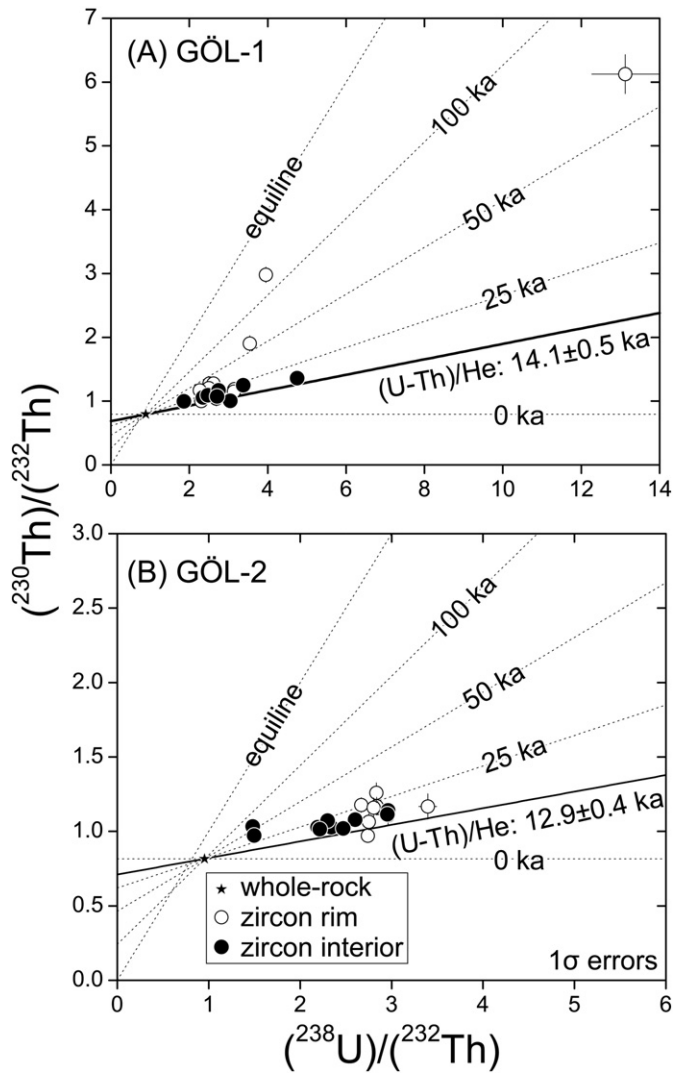


**Fig. 2.** U–Th isochron diagram for Gölcük intracaldera dome zircon and whole-rock samples GÖL-1 (A) and GÖL-2 (B). Model isochron ages are fixed at the whole-rock composition and shown for ages of 0, 25, 50, and 100 ka and secular equilibrium (dashed lines), as well as the model isochron corresponding to the (U–Th)/He zircon age (solid lines).

methods such as cosmogenic dating (e.g., Schmitt et al., 2010a) and  $^{14}\text{C}$  (e.g., Danišik et al., 2012). The disequilibrium-corrections applied here are based on measured rim ages for the same crystals that were analyzed for (U–Th)/He. There is a possibility that U–Th zonation and compositional heterogeneities (e.g., Dobson et al., 2008) could introduce bias in (U–Th)/He ages. However, the lack of systematic age and U abundance relations between rims and interiors for Gölcük zircons (Fig. 3) implies that any systematic biases are unlikely, and well within our stated uncertainties. Moreover, if crystals interiors were significantly older than the rim ages, the resulting corrections for initial  $^{230}\text{Th}$  deficit would become smaller (Fig. 4), and the age differences between (U–Th)/He and K–Ar would increase. The causes for the discrepancy between (U–Th)/He and K–Ar ( $^{40}\text{Ar}/^{39}\text{Ar}$ ) eruption ages remain speculative: post-eruptive re-heating of the lavas causing  $^4\text{He}$ -loss from zircon is implausible because the intracaldera domes represent the youngest eruptions and they are not in contact with younger rocks. Heterogeneity in  $^{40}\text{Ar}/^{39}\text{Ar}$  K-feldspar ages indicates that the magmas incorporated crystals that significantly predate the eruption. This or other forms of excess  $^{40}\text{Ar}$  in mesostasis and K-feldspar could lead to unrecognized age overestimation.

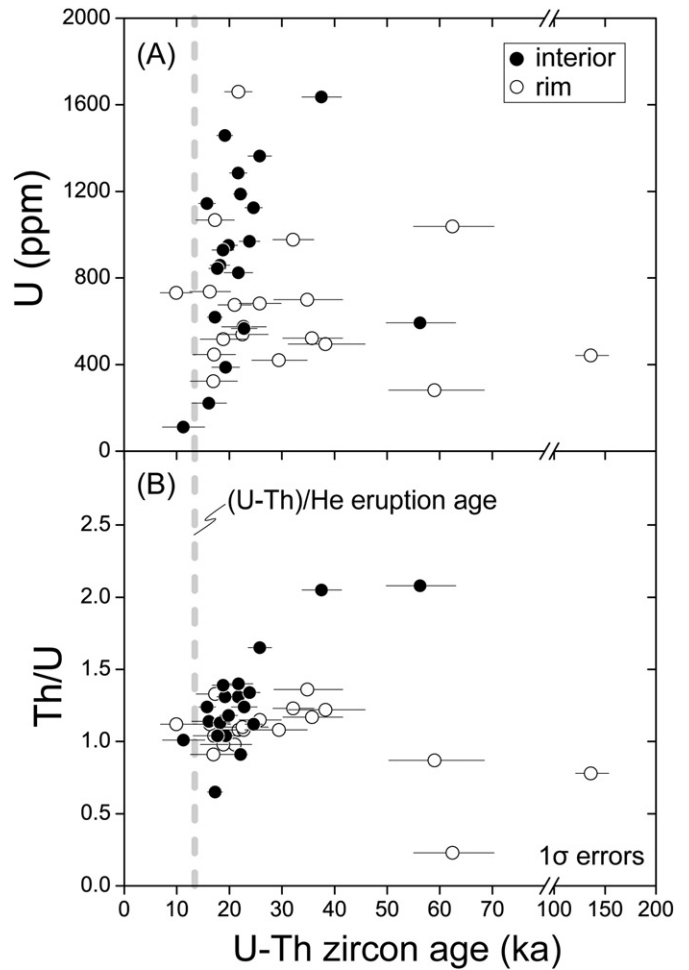


**Fig. 3.** U abundances (A) and Th/U (B) vs. age for zircon crystals from Gölcük intracaldera domes.

### 5.2. Zircon origins in Gölcük lavas

U–Th zircon age probability density distributions are polymodal, with a major peak at ca. 20 ka, and minor peaks (in decreasing abundance) at ca. 37, 59, and 136 ka (Fig. 5). Interestingly, both zircon rims and interiors peak at ~20 ka, and older ages exist among rims and interiors (note that rim and interior ages are for different crystals). Probability density curves for rim and core ages populations are very similar, and do not permit to resolve rim-core age zonation (Fig. 5). Instead, Gölcük zircon crystals comprise age populations that crystallized at different times, but lack strong internal age zonation. This could imply that zircon crystals in the intracaldera lavas were carried over from intrusive rocks generated during earlier magmatic cycles, but did not reside in the host magma sufficiently long to crystallize a near-eruption aged rim. Zircon carry-over is supported by the recently reported rare presence of zircon in cycle I rocks, and in monzosyenite plutonic xenoliths of explosive cycle III rocks (Platevoet et al., 2014). It is thus conceivable that antecrystic zircons represent remnants of differentiated plutonic rocks from earlier magmatic pulses which may or may not have erupted zircon-bearing rocks. Syenitic plutonic enclaves from the Breccia Museo (Campi Flegrei), for example, contain zircon (Gebauer et al., 2014), whereas juvenile pumice of the co-erupted Campanian Ignimbrite is largely devoid of zircon. The minor peak at ca. 59 ka overlaps with K–Ar and  $^{40}\text{Ar}/^{39}\text{Ar}$  ages that Platevoet et al. (2008) assigned to the Gölcük cycle II, but this might be coincidental because of the doubtful age relevance of these data.

Antecrystic zircons at Gölcük make up only a small portion of the overall zircon population. For most zircons, the difference between

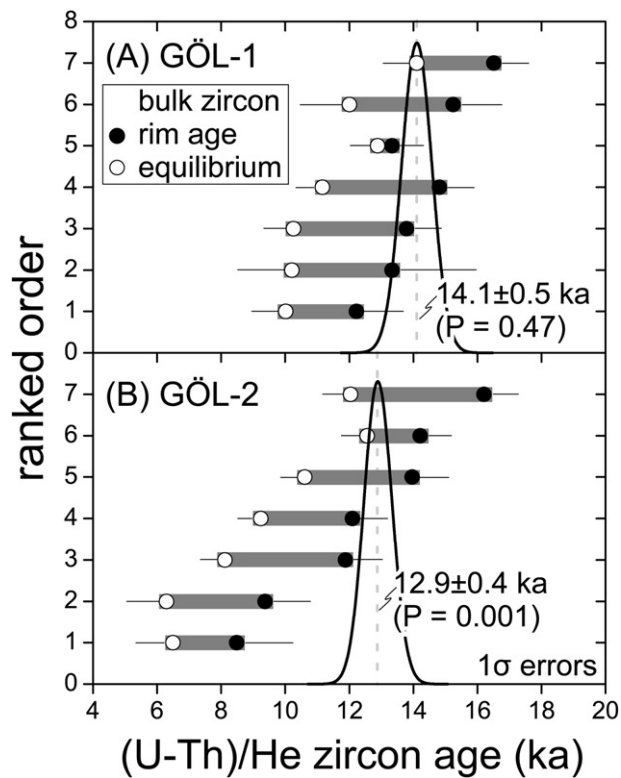


**Fig. 4.** (U–Th)/He zircon ages for Gölcük intracaldera domes showing equilibrium (open circles) and disequilibrium-corrected (based on the U–Th zircon rim age; solid circles) ages. Connecting thick gray bar outlines the theoretically permissible range of disequilibrium in (U–Th)/He ages; thin black bar indicates analytical uncertainty. Because rim and interior ages are indistinguishable (Fig. 2) and zircon crystals thus likely unzoned with regard to age, the (U–Th)/He age corrections based on the rim ages is more favored here. The rim-age disequilibrium corrected (U–Th)/He ages are shown in the probability curves and vertical bar (average).

the peak in the U–Th zircon disequilibrium age distribution and the (U–Th)/He eruption age imply short pre-eruptive crystal residence times, on the order of several ka. For typical crystal dimensions of Gölcük zircons (radii between ~50 and 100  $\mu\text{m}$ ), these durations translate into zircon crystallization rates of  $\sim 10^{-13}$  to  $10^{-14}$  cm/a

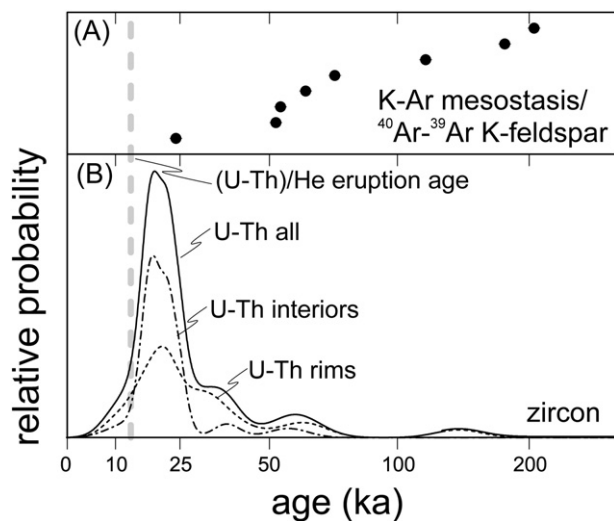


**Fig. 5.** Comparison of published K–Ar and  $^{40}\text{Ar}/^{39}\text{Ar}$  ages on mesostasis and K-feldspar, respectively (A; Platevoet et al., 2008) with U–Th zircon crystallization ages and the average (U–Th)/He eruption age for Gölcük intracaldera domes (B; this study). U–Th rim and core ages are statistically equivalent at a probability  $P = 0.29$ , which is significantly higher than the rejection criterion for the hypothesis that both populations are identical of  $P = 0.05$ .

which agree with rates predicted from diffusion modeling (Watson, 1996) and those empirically observed based on U–Th disequilibrium geochronology (e.g., Storm et al., 2011; Schmitt et al., 2011).

Comparatively brief pre-eruptive zircon residence times at Gölcük differ from many other continental and oceanic arc magmas where crystallization ages in individual lava or pumice samples frequently record pre-eruptive zircon residence over 10's to 100's of ka (e.g., Claiborne et al., 2010; Schmitt et al., 2010b). The comparatively scarce antecrystic zircons at Gölcük and a complete lack of crystals predating the eruption by 100's of ka (i.e., from the Pleistocene cycle I; Platevoet et al., 2008), may reflect the prevalence of alkaline and mafic magmas in the Gölcük magma system. Such compositions are unfavorable to the crystallization of zircon (e.g., Boehnke et al., 2013), and thus prone to rapid resorption of pre-existing zircon. The U–Th zircon crystallization age spectra of the most recent Gölcük lavas may thus underestimate the overall longevity of the magma system; additional studies of zircon in plutonic xenoliths erupted at Gölcük (Platevoet et al., 2014) have the potential to fill this gap.

## 6. Conclusions

(U–Th)/He zircon eruption ages for two intracaldera lava domes indicate that Gölcük volcano was last active near the Pleistocene–Holocene boundary and suggest that Gölcük is a dormant volcano. Overlapping (U–Th)/He ages for these lavas of  $14.1 \pm 0.5$  and  $12.9 \pm 0.4$  ka do not support separate intracaldera effusive eruptions implied by data of Platevoet et al. (2008). Young (U–Th)/He zircon ages open the possibility for a much younger age for the preceding caldera-forming eruption than previously proposed based on K–Ar dating. U–Th zircon crystallization ages also indicate nearly-continuous magma presence for at least several ka prior to eruption. Zircon evidence for protracted magma presence, albeit shorter than in many long-lived silicic arc volcanoes, implies that the Gölcük magma system has potential for future eruptions.

## Acknowledgments

We acknowledge the assistance of Janet C. Harvey and Felix Wicke during fieldwork, Simone Jahn for help in zircon separation, and Noreen Evans (Curtin University), Cam Scadding and Allen Thomas (TSW Analytical, Perth) for assistance with ICP MS analyses. This study was supported by a grant from the German Science Foundation DFG (Si 718/9-1). The ion microprobe facility at UCLA is partly supported by a grant from the Instrumentation and Facilities Program, Division of Earth Sciences, National Science Foundation. Uranium and thorium isotopic determination by MC-ICP-MS was supported by Taiwan MOST (102-2116-M-002-016, 102-3113-P-002-011, 103-2119-M-002-022) and NTU (101R7625) grants.

## Appendix A. Supplementary data

Supplementary data to this article can be found online at <http://dx.doi.org/10.1016/j.jvolgeores.2014.08.027>.

## References

- Alici, P., Temel, A., Gourgaud, A., Kieffer, G., Gündoğdu, M.N., 1998. Petrology and geochemistry of potassic rocks in the Gölcük area (Isparta, SW Turkey): genesis of enriched alkaline magmas. *J. Volcanol. Geotherm. Res.* 85 (1), 423–446.
- Boehnke, P., Watson, E.B., Trail, D., Harrison, T.M., Schmitt, A.K., 2013. Zircon saturation revisited. *Chem. Geol.* 351, 324–334.
- Cheng, H., Edwards, R.L., Shen, C.-C., Polyak, V.J., Asmerom, Y., Woodhead, J., Hellstrom, J., Wang, Y., Kong, X., Spötl, C., Wang, X., Alexander Jr., E.C., 2013. Improvements in  $^{230}\text{Th}$  dating,  $^{230}\text{Th}$  and  $^{234}\text{U}$  half-life values, and U–Th isotopic measurements by multi-collector inductively coupled plasma mass spectrometry. *Earth Planet. Sci. Lett.* 371, 82–91.
- Claiborne, L.L., Miller, C.F., Flanagan, D.M., Clynne, M.A., Wooden, J.L., 2010. Zircon reveals protracted magma storage and recycling beneath Mount St. Helens. *Geology* 38 (11), 1011–1014.

- Danišik, M., Shane, P., Schmitt, A.K., Hogg, A., Santos, G.M., Storm, S., Evans, N.J., Fifield, L.K., Lindsay, J.M., 2012. Re-anchoring the late Pleistocene tephrochronology of New Zealand based on concordant radiocarbon ages and combined  $^{238}\text{U}/^{230}\text{Th}$  disequilibrium and (U–Th)/He zircon ages. *Earth Planet. Sci. Lett.* 349, 240–250.
- Dilek, Y., Sandvol, E., 2009. Seismic structure, crustal architecture and tectonic evolution of the Anatolian–African plate boundary and the Cenozoic orogenic belts in the Eastern Mediterranean region. *Geol. Soc. Lond. Spec. Publ.* 327 (1), 127–160.
- Dilek, Y., Imamverdiyev, N., Altunkaynak, Ş., 2010. Geochemistry and tectonics of Cenozoic volcanism in the Lesser Caucasus (Azerbaijan) and the peri-Arabian region: collision-induced mantle dynamics and its magmatic fingerprint. *Int. Geol. Rev.* 52 (4–6), 536–578.
- Dobson, K.J., Stuart, F.M., Dempster, T.J., EIMF, 2008. U and Th zonation in Fish Canyon Tuff zircons: implications for a zircon (U–Th)/He standard. *Geochim. Cosmochim. Acta* 72 (19), 4745–4755.
- Elitok, Ö., Özgür, N., Drüppel, K., Dilek, Y., Platevoet, B., Guillou, H., Poisson, A., Scaillet, S., Satir, M., Siebel, W., Bardintzeff, J.-M., Deniel, C., Yilmaz, K., 2010. Origin and geodynamic evolution of late Cenozoic potassium-rich volcanism in the Isparta area, southwestern Turkey. *Int. Geol. Rev.* 52 (4–6), 454–504.
- Farley, K.A., Wolf, R.A., Silver, L.T., 1996. The effects of long alpha-stopping distances on (U–Th)/He ages. *Geochim. Cosmochim. Acta* 60 (21), 4223–4229.
- Farley, K.A., Kohn, B.P., Pillans, B., 2002. The effects of secular disequilibrium on (U–Th)/He systematics and dating of Quaternary volcanic zircon and apatite. *Earth Planet. Sci. Lett.* 201 (1), 117–125.
- Gebauer, S.K., Schmitt, A.K., Pappalardo, L., Stockli, D.F., Lovera, O.M., 2014. Crystallization and eruption ages of Breccia Museo (Campi Flegrei caldera, Italy) plutonic clasts and their relation to the Campanian ignimbrite. *Contrib. Mineral. Petrol.* 167 (1), 1–18.
- Hoskin, P.W., Schaltegger, U., 2003. The composition of zircon and igneous and metamorphic petrogenesis. *Rev. Mineral. Geochem.* 53 (1), 27–62.
- Hourigan, J.K., Reiners, P.W., Brandon, M.T., 2005. U–Th zonation-dependent  $\alpha$ -ejection in (U–Th)/He chronometry. *Geochim. Cosmochim. Acta* 69, 3349–3365.
- Lefèvre, C., Bellon, H., Poisson, A., 1983. Présences de leucitites dans le volcanisme Pliocène de la région d'Isparta (Taurides occidentales, Turquie). *C. R. Acad. Sci. Hebd. Seances Acad. Sci. D* 297 (2), 367–372.
- Platevoet, B., Scaillet, S., Guillou, H., Blamart, D., Nomade, S., Massault, M., Poisson, A., Elitok, Ö., Nevzat, Ö., Yagmurlu, F., Yilmaz, K., 2008. Pleistocene eruptive chronology of the Gölcük volcano, Isparta Angle, Turkey. *Quaternaire* 19 (2), 147–156.
- Platevoet, B., Elitok, Ö., Guillou, H., Bardintzeff, J.M., Yagmurlu, F., Nomade, S., Poisson, A., Deniel, C., Özgür, N., 2014. Petrology of Quaternary volcanic rocks and related plutonic xenoliths from Gölcük volcano, Isparta Angle, Turkey: origin and evolution of the high-K alkaline series. *J. Asian Earth Sci.* 92, 53–76.
- Press, W.H., Teukolsky, S.A., Vetterling, W.T., Flannery, B.P., 2002. *Numerical Recipes: The Art of Scientific Computing*. Cambridge University Press, New York.
- Schmitt, A.K., 2007. Ion microprobe analysis of ( $^{231}\text{Pa}$ )/( $^{235}\text{U}$ ) and an appraisal of protactinium partitioning in igneous zircon. *Am. Mineral.* 92 (4), 691–694.
- Schmitt, A.K., Stockli, D.F., Niedermann, S., Lovera, O.M., Hausback, B.P., 2010a. Eruption ages of Las Tres Virgenes volcano (Baja California): a tale of two helium isotopes. *Quat. Geochronol.* 5 (5), 503–511.
- Schmitt, A.K., Stockli, D.F., Lindsay, J.M., Robertson, R., Lovera, O.M., Kislitsyn, R., 2010b. Episodic growth and homogenization of plutonic roots in arc volcanoes from combined U–Th and (U–Th)/He zircon dating. *Earth Planet. Sci. Lett.* 295 (1), 91–103.
- Schmitt, A.K., Danišik, M., Evans, N.J., Siebel, W., Kiemele, E., Aydin, F., Harvey, J.C., 2011. Acıgöl rhyolite field, Central Anatolia (part 1): high-resolution dating of eruption episodes and zircon growth rates. *Contrib. Mineral. Petrol.* 162 (6), 1215–1231.
- Shen, C.-C., Edwards, R.L., Cheng, H., Dorale, J.A., Thomas, R.B., Bradley Moran, S., Weinstein, S.E., Edmonds, H.N., 2002. Uranium and thorium isotopic and concentration measurements by magnetic sector inductively coupled plasma mass spectrometry. *Chem. Geol.* 185 (3), 165–178.
- Shen, C.-C., Cheng, H., Edwards, R.L., Moran, S.B., Edmonds, H.N., Hoff, J.A., Thomas, R.B., 2003. Measurement of attogram quantities of  $^{231}\text{Pa}$  in dissolved and particulate fractions of seawater by isotope dilution thermal ionization mass spectroscopy. *Anal. Chem.* 75 (5), 1075–1079.
- Shen, C.-C., Wu, C.-C., Cheng, H., Edwards, R.L., Hsieh, Y.-T., Gallet, S., Chang, C.-C., Li, T.-Y., Lam, D.D., Kano, A., Hori, M., Spötl, C., 2012. High-precision and high-resolution carbonate  $^{230}\text{Th}$  dating by MC-ICP-MS with SEM protocols. *Geochim. Cosmochim. Acta* 99, 71–86.
- Storm, S., Shane, P., Schmitt, A.K., Lindsay, J.M., 2011. Decoupled crystallization and eruption histories of the rhyolite magmatic system at Tarawera volcano revealed by zircon ages and growth rates. *Contrib. Mineral. Petrol.* 163 (3), 505–519.
- Watson, E.B., 1996. Dissolution, growth and survival of zircons during crustal fusion: kinetic principals, geological models and implications for isotopic inheritance. *Trans. R. Soc. Edinb. Earth Sci.* 87 (1–2), 43–56.